

Research Article
Implant Science



OPEN ACCESS

Received: Jan 17, 2020

Revised: Apr 1, 2020

Accepted: Apr 20, 2020

***Correspondence:**

Daniel S. Thoma

Clinic of Reconstructive Dentistry, University of Zurich, Zurich, Switzerland, Center of Dental Medicine, University of Zürich, Plattenstrasse 11 CH-8032 Zürich, Switzerland.

E-mail: daniel.thoma@zzm.uzh.ch

Tel: +41 44 634 32 52

Fax: +41 44 634 43 05

Copyright © 2020. Korean Academy of Periodontology

This is an Open Access article distributed under the terms of the Creative Commons Attribution Non-Commercial License (<https://creativecommons.org/licenses/by-nc/4.0/>).

ORCID iDs

Nadja Naenni

<https://orcid.org/0000-0002-6689-2684>

Hyun-Chang Lim

<https://orcid.org/0000-0001-7695-1708>

Franz-Josef Strauss

<https://orcid.org/0000-0002-5832-7327>

Ronald E. Jung

<https://orcid.org/0000-0003-2055-1320>

Christoph H. F. Hämmerle

<https://orcid.org/0000-0002-8280-7347>

Daniel S. Thoma

<https://orcid.org/0000-0002-1764-7447>

Author Contributions

Conceptualization: Daniel S. Thoma; Formal analysis: Franz-Josef Strauss; Investigation: Daniel S. Thoma, Nadja Naenni; Methodology: Daniel S. Thoma, Nadja Naenni; Project administration: Daniel S. Thoma; Writing - original draft: Hyun-Chang Lim, Nadja Naenni,

Local tissue effects of various barrier membranes in a rat subcutaneous model

Nadja Naenni ¹, **Hyun-Chang Lim** ², **Franz-Josef Strauss** ^{1,3,4},
Ronald E. Jung ¹, **Christoph H. F. Hämmerle** ¹, **Daniel S. Thoma** ^{1,5,*}

¹Clinic of Reconstructive Dentistry, University of Zurich, Zurich, Switzerland

²Department of Periodontology, Periodontal-Implant Clinical Research Institute, Kyung Hee University School of Dentistry, Seoul, Korea

³Department of Conservative Dentistry, University of Chile, School of Dentistry, Santiago, Chile

⁴Department of Oral Biology, Medical University of Vienna, School of Dentistry, Vienna, Austria

⁵Department of Periodontology, Research Institute for Periodontal Regeneration, Yonsei University College of Dentistry, Seoul, Korea

ABSTRACT

Purpose: The purpose of this study was to examine the local tissue reactions associated with 3 different poly(lactic-co-glycolic acid) (PLGA) prototype membranes and to compare them to the reactions associated with commercially available resorbable membranes in rats.

Methods: Seven different membranes—3 synthetic PLGA prototypes (T1, T2, and T3) and 4 commercially available membranes (a PLGA membrane, a poly[lactic acid] membrane, a native collagen membrane, and a cross-linked collagen membrane)—were randomly inserted into 6 unconnected subcutaneous pouches in the backs of 42 rats. The animals were sacrificed at 4, 13, and 26 weeks. Descriptive histologic and histomorphometric assessments were performed to evaluate membrane degradation, visibility, tissue integration, tissue ingrowth, neovascularization, encapsulation, and inflammation. Means and standard deviations were calculated.

Results: The histological analysis revealed complete integration and tissue ingrowth of PLGA prototype T1 at 26 weeks. In contrast, the T2 and T3 prototypes displayed slight to moderate integration and tissue ingrowth regardless of time point. The degradation patterns of the 3 synthetic prototypes were similar at 4 and 13 weeks, but differed at 26 weeks. T1 showed marked degradation at 26 weeks, whereas T2 and T3 displayed moderate degradation. Inflammatory cells were present in all 3 prototype membranes at all time points, and these membranes did not meaningfully differ from commercially available membranes with regard to the extent of inflammatory cell infiltration.

Conclusions: The 3 PLGA prototypes, particularly T1, induced favorable tissue integration, exhibited a similar degradation rate to native collagen membranes, and elicited a similar inflammatory response to commercially available non-cross-linked resorbable membranes. The intensity of inflammation associated with degradable dental membranes appears to relate to their degradation kinetics, irrespective of their material composition.

Keywords: Guided tissue regeneration; Bone regeneration; Materials testing; Poly(lactic acid-polyglycolic acid) copolymer; Dental implants

Daniel S. Thoma, Ronald E. Jung, Franz-Josef Strauss; Writing - review & editing: Hyun-Chang Lim, Nadja Naenni, Franz-Josef Strauss, Daniel S. Thoma, Ronald E. Jung, Christoph H. F. Hämmerle.

Conflict of Interest

No potential conflict of interest relevant to this article was reported.

INTRODUCTION

As the number of dental implants that can be placed in a prosthetically ideal position has increased, simultaneous hard tissue augmentation has become a common procedure in dental practice. According to the dental literature, approximately 40% of implant treatments require hard tissue augmentation [1]. Various methods have been proposed, of which guided bone regeneration (GBR) is the treatment modality applied most often [2-4].

GBR involves the selective repopulation of a defect site with osteoprogenitor cells, which is conducted by positioning a physical barrier membrane between the hard tissue defect and the adjacent soft tissues [5,6]. Various types of membranes, including non-resorbable and resorbable membranes, have been utilized. In the early days of GBR research, non-resorbable barrier membranes were considered to be the gold standard. This type of membrane, however, requires a second surgical procedure for its removal. Moreover, several studies have found that non-resorbable membranes are associated with a relatively high risk of membrane exposure and high subsequent infection rates [7-9]. To overcome these drawbacks, resorbable membranes have become more frequently used than non-resorbable membranes. Resorbable membranes do not require a second procedure and, if exposed, are still able to support wound healing without premature removal of the membrane [10]. Despite these clinical advantages, resorbable membranes have some limitations, such as low space-maintenance capability and variable resorption [11]. Consequently, extensive research has been conducted to investigate ways to improve or modify the physicochemical properties of these membranes using different compositions of materials.

Resorbable membranes can be composed of natural polymers, synthetic polymers, or inorganic compounds [12]. Among the natural polymers, collagen-based membranes are the most commonly used for GBR procedures. These are mainly derived from animal tissues, and their degradation largely depends on the animal source [11] and thus cannot be controlled. This is of particular importance, since membranes that exhibit early degradation may not persist for the duration needed for optimal tissue regeneration. To slow the process of degradation, physicochemical methods such as cross-linking have been utilized to enhance collagen membrane stability [13].

In addition to collagen membranes, resorbable membranes based on synthetic polymers have been introduced. These membranes are made from aliphatic polyesters such as poly(lactic acid) (PLA) and poly(lactic-co-glycolic acid) (PLGA) [12]. The main advantages of these membranes are their manageability, the potential of influencing their biodegradation, and the lack of associated cross-infections [14,15]. However, they may impair bone healing at the augmented site due to adverse inflammatory tissue reactions [16]. Consequently, various modifications of synthetic polymers have been made to attempt to prevent this issue. These modifications may alter the degradation time, tissue integration, extent of inflammation, and, eventually, the clinical outcomes.

Considering that a newly developed membrane should pass a series of evaluations before its clinical application, the aim of the present study was to investigate local tissue reactions to 3 PLGA prototype membranes in comparison with commercially available resorbable membranes in a rat subcutaneous implantation model.

MATERIALS AND METHODS

Study design

The present study was designed as a randomized controlled experimental preclinical trial in compliance with the International Organization for Standardization (ISO) 10993-6 standards for investigating local tissue effects after subcutaneous implantation. The study was conducted according to Organization for Economic Cooperation and Development and US Food and Drug Administration Good Laboratory Practice regulations in an accredited and registered animal facility. The approval of the local NAMSA Ethical Committee was obtained prior to the beginning of the study. The animals were kept under standard conditions in a purpose-designed room for experimental animals. All animals were treated according to the Animals in Research: Reporting *In Vivo* Experiments guidelines for animal care, with free access to water and a standard diet.

Animals

Forty-two rats (mass, 272–333 g) of the Sprague-Dawley strain (Charles River Laboratories, Écully, France) were used in this study. Fourteen rats were randomly allocated to each of 3 observation time points (4, 13, and 26 weeks) using a computer-generated randomization list.

Study materials

Seven different barrier membranes were applied:

- T1: synthetic PLGA prototype T1 (Sunstar Suisse SA, Etoy, Switzerland)
- T2: synthetic PLGA prototype T2 (Sunstar Suisse SA)
- T3: synthetic PLGA prototype T3 (Sunstar Suisse SA)
- PLGA-C1: commercially available PLGA membrane (Tisseos[®]; Biomedical Tissues, La Chapelle-sur-Erdre, France)
- PLA-C2: synthetic PLA membrane (GUIDOR[®]; Guidor AB, Huddinge, Sweden)
- NCM-C3: native collagen membrane (Bio-Gide[®]; Geistlich Pharma AG, Wolhusen, Switzerland)
- CLCM-C4: cross-linked collagen membrane (Ossix Plus[®]; Regedent AG, Zurich, Switzerland)
- Negative control (NC): high-density polyethylene membrane

Surgical procedure

The surgical procedure was performed as previously described with some minor modifications [17]. In brief, the animals were anesthetized via inhalation of 1.5% isoflurane (Forane[®]; Baxter Healthcare Corp., Deerfield, IL, USA). An area approximately 8 cm in length and 4 cm in width was depilated on the back of each rat. A skin incision was made, and 6 unconnected subcutaneous pouches were prepared. Each membrane was cut to a diameter of 10 mm with a biopsy punch and marked with a single knot suture to allow for later re-discovery of the membrane. The membranes were then randomly placed in the pouches according to a computer-generated randomization list. The incisions were closed using stainless steel wound clips. For pain relief, buprenorphine (Buprecare[®]; Axience, Pantin, France) was administered at the end of the procedure and then twice a day following surgery. The stainless-steel wound clips were removed 2 weeks after surgery. The rats were housed in cages under standard conditions during the time of the investigation.

Sacrifice

At 4, 13, and 26 weeks (n=14 per time point), the animals were anesthetized with an intramuscular injection of tiletamine zolazepam (Zoletil®; Virbac, Carros, France) and were then euthanized with an intravenous injection of pentobarbital (Dolethal; Vetoquinol, Lure, France). Collagen membrane residues were removed along with the surrounding connective tissue and fixed in 10% buffered formalin.

Histological and histomorphometric analyses

A total of 252 samples were obtained (84 samples per time point), and at least 10 samples per membrane and time point were further processed. After fixation, each of the 252 samples was dehydrated in a series of alcohol solutions of increasing concentration and was subsequently embedded in paraffin. Samples were cut to 4.5 µm using a microtome. Two central sections per block were prepared. One section was stained with modified Masson's trichrome stain and the other with safranin-hematoxylin-eosin. All samples were prepared in a standard manner according to the ISO 10993-6 guidelines. The local tissue effects and the inflammatory response at the implantation sites were then scored semi-quantitatively and descriptively by a single pathologist who was not involved in the sample preparation and was thus blinded to the different groups. The following parameters were evaluated descriptively at each time point: visibility of the membrane, material degradation, neovascularization, tissue integration, tissue ingrowth, and inflammation. The measurements were scored according to the ISO 10993-6 guidelines: 0, none; 1, slight; 2, moderate; 3, marked; and 4, complete/severe. Neovascularization was scored according to the capillaries present: 0, none; 1, minimal capillary proliferation; 2, groups of 4–7 capillary structures; 3, a broad band of capillaries; and 4, an extensive band of capillaries. Inflammation was descriptively assessed according to the number of macrophages, polymorphonuclear cells, lymphocytes, and giant cells present. In addition, encapsulation was descriptively evaluated according to the concentric organization of mature collagen around the membranes, with the following scoring system: 0, none; 1, a narrow band; 2, a moderate band; 3, a thick band; and 4, an extensive band.

Statistical analysis

Descriptive statistics for all variables are shown in Tables 1 and 2 as mean±standard deviation. The visibility and degradation score of each membrane are presented graphically using line

Table 1. Histopathologic evaluation

Time point (weeks)	Scoring grade											
	T1			T2			T3			NCM-C3		
	4 weeks	13 weeks	26 weeks	4 weeks	13 weeks	26 weeks	4 weeks	13 weeks	26 weeks	4 weeks	13 weeks	26 weeks
Neovascularization	1.7±0.4	2.0±0.0	1.4±0.5	0.4±0.5	0.5±0.5	1.4±0.5	0.6±0.5	0.8±0.4	1.0±0.0	1.6±0.5	1.0±0.0	1.0±0.0
Tissue integration ^{a)}	2.0±0.0	3.0±0.4	4.0±0.0	1.0±0.0	1.0±0.0	1.5±0.5	1.0±0.0	1.6±0.5	2.1±0.5	1.9±0.3	2.9±0.3	4.0±0.0
Encapsulation ^{b)}	1.8±0.4	1.0±0.6	0.0±0.0	1.0±0.0	2.0±2.0	1.4±0.5	1.0±0.0	1.1±0.6	1.2±0.6	0.8±0.6	0.1±0.3	0.0±0.0
Tissue ingrowth ^{c)}	3.3±0.7	3.1±0.3	4.0±0.0	1.0±0.0	1.0±0.0	1.6±0.5	1.0±0.0	1.6±0.5	2.3±0.6	2.3±0.6	2.0±0.0	4.0±0.0
Neovascularization	2.8±0.4	2.1±0.3	1.8±0.4	2.0±0.0	2.0±0.0	1.9±0.3	0.0±0.0	0.2±0.6	0.0±0.0	2.0±0.0	2.1±0.3	0.1±0.3
Tissue integration	2.8±0.6	4.0±0.0	4.0±0.0	2.0±0.4	3.0±0.0	2.9±0.3	0.0±0.0	1.0±0.0	0.9±0.3	0.0±0.0	0.0±0.0	0.0±0.0
Encapsulation	1.1±0.5	0.0±0.0	0.0±0.0	0.8±0.4	1.9±0.3	1.9±0.3	2.0±0.0	2.0±0.0	2.0±0.0	2.0±0.0	2.0±0.0	1.1±0.3
Tissue ingrowth	2.8±0.6	4.0±0.0	4.0±0.0	2.1±0.3	4.0±0.0	4.0±0.0	0.0±0.0	0.3±0.7	0.2±0.4	0.0±0.0	0.0±0.0	0.0±0.0

Numbers represent the mean±standard deviation of the parameters using the following scoring system: 0=none, 1=slight, 2=moderate, 3=marked, and 4=complete/severe.

PLGA: poly(lactic-co-glycolic acid), PLA: poly(lactic acid), T1: synthetic PLGA prototype test 1, T2: synthetic PLGA prototype test 2, T3: synthetic PLGA prototype test 3, NCM-C3: native collagen membrane, PLGA-C1: commercially available PLGA membrane, PLA-C2: synthetic PLA membrane, CLCM-C4: cross-linked collagen membrane, NC: negative control.

^{a)}Process whereby no reactive tissues create a barrier between host tissues and the membrane. ^{b)}Concentric organization of mature collagen deposits that tend to isolate the membrane from the host tissues. ^{c)}Growth of tissues inward or into the implanted membrane.

Table 2. Histopathologic evaluation of inflammation

Time point (weeks)	Scoring grade											
	T1			T2			T3			NCM-C3		
	4 weeks	13 weeks	26 weeks	4 weeks	13 weeks	26 weeks	4 weeks	13 weeks	26 weeks	4 weeks	13 weeks	26 weeks
Polymorphonuclear cells	0.1±0.3	0.0±0.0	0.0±0.0	1.0±0.0	0.2±0.4	0.2±0.4	0.9±0.3	0.0±0.0	0.0±0.0	0.9±0.3	0.0±0.0	0.1±0.3
Lymphocytes	0.5±0.5	0.9±0.5	0.8±0.5	0.3±0.5	0.9±0.3	0.9±0.5	0.3±0.4	0.7±0.5	0.8±0.4	1.9±0.9	0.5±0.5	0.5±0.7
Macrophages	2.5±0.5	2.4±0.5	1.6±0.5	2.0±0.0	2.0±0.0	1.8±0.4	2.0±0.0	1.8±0.4	2.3±0.7	1.6±0.5	1.0±0.0	1.0±0.0
Giant cells	2.7±0.6	2.9±0.3	1.3±0.5	2.0±0.0	1.9±0.3	1.3±0.4	2.0±0.0	2.1±0.3	1.8±0.7	1.8±0.9	0.0±0.0	0.2±0.4
Polymorphonuclear cells	0.9±0.3	0.2±0.4	0.0±0.0	0.7±0.5	0.6±0.5	0.3±0.4	0.0±0.0	0.0±0.0	0.0±0.0	1.0±0.0	0.3±0.5	0.4±0.5
Lymphocytes	0.2±0.4	1.2±0.4	0.6±0.5	0.9±0.3	0.9±0.3	1.0±0.4	0.7±0.5	0.2±0.6	0.1±0.3	0.8±0.4	0.9±0.5	0.4±0.5
Macrophages	2.7±0.6	2.0±0.4	2.0±0.0	1.3±0.5	1.8±0.4	3.0±0.0	1.0±0.0	1.1±0.3	1.0±0.0	1.3±0.5	1.3±0.5	1.1±0.3
Giant cells	2.8±0.6	2.8±0.6	1.9±0.3	1.2±0.4	1.8±0.4	2.2±0.4	0.1±0.3	0.2±0.4	0.0±0.0	0.6±0.5	0.9±0.3	0.5±0.5

Numbers represent the mean±standard deviation of inflammatory cell infiltration using the following scoring system: 0=none, 1=slight, 2=moderate, 3=marked, and 4=complete/severe.

PLGA: poly(lactic-co-glycolic acid), PLA: poly(lactic acid), T1: synthetic PLGA prototype test 1, T2: synthetic PLGA prototype test 2, T3: synthetic PLGA prototype test 3, NCM-C3: native collagen membrane, PLGA-C1: commercially available PLGA membrane, PLA-C2: synthetic PLA membrane, CLCM-C4: cross-linked collagen membrane, NC: negative control.

charts. The sample size adhered to the ISO 10993-6 standards for assessment of local tissue effects after implantation.

RESULTS

All 42 rats remained healthy during the entire study period. In general, all membranes became integrated into the surrounding soft tissues except for CLCM-C4 and the NC. The density of the newly formed connective tissue gradually increased over the observational period. In contrast, the collagen and synthetic networks decreased in density to varying degrees over time. Inflammatory cells were present in all membranes at all time points to varying extents.

Histopathologic evaluation

Visibility

At 4 weeks, the histological analysis revealed that the majority of membranes were consistently visible (Figure 1). At 13 weeks, the visibility levels of some of the membranes were reduced, particularly NCM-C3. At 26 weeks, NC, CLCM-C4, PLA-C2, T3, and T2 were still frequently detectable; however, T1, PLGA-C1, and NCM-C3 were barely visible.

Degradation

At 4 weeks, 2 membranes—PLGA-C1 and NCM-C3—displayed slight degradation (Figure 2). At 13 weeks, all membranes showed slight to moderate degradation except the CLCM-C4 membrane and the NC. After a healing period of 26 weeks, most of the membranes exhibited greater degradation than before, particularly T1 and NCM-C3, which showed marked degradation. Nonetheless, CLCM-C4 and NC still did not display clear signs of degradation.

Tissue integration

At 4 weeks, all membranes displayed slight to moderate tissue integration except for CLCM-C4 and NC (Figure 3A and Table 1). At 13 weeks, tissue integration was more distinct in all membranes than it was at the earlier time point, particularly for PLGA-C1, which demonstrated complete tissue integration. At 26 weeks, T1, NCM-C3, and PLGA-C1 exhibited complete tissue integration, while T2, T3, and PLA-C2 showed moderate to marked tissue

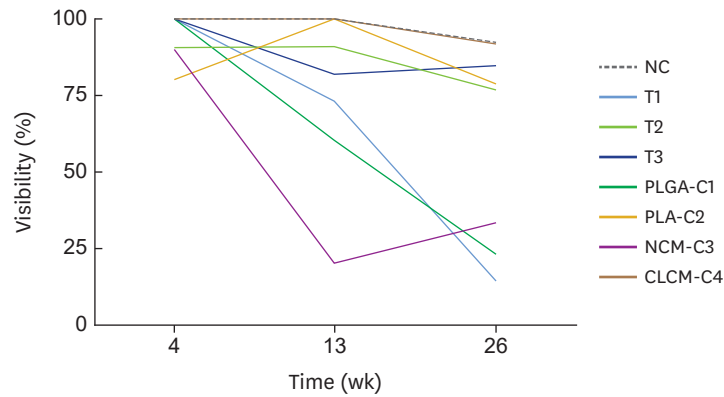


Figure 1. Visibility of the membranes over time.

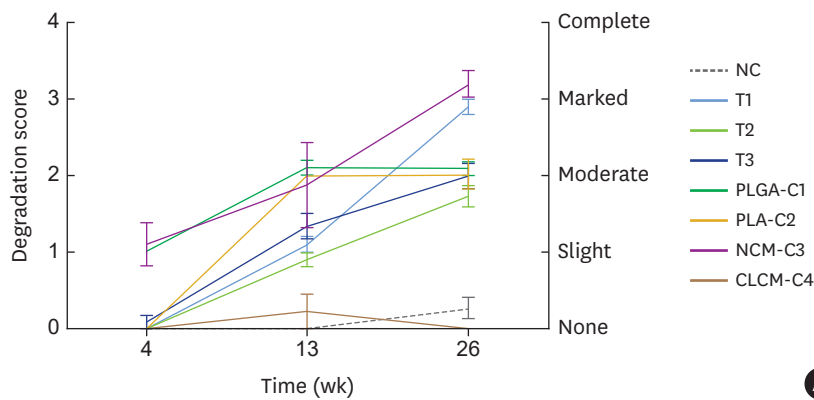
Data represent the means.

PLGA: poly(lactic-co-glycolic acid), PLA: poly(lactic acid), NC: negative control, T1: synthetic PLGA prototype test 1, T2: synthetic PLGA prototype test 2, T3: synthetic PLGA prototype test 3, PLGA-C1: commercially available PLGA membrane, PLA-C2: synthetic PLA membrane, NCM-C3: native collagen membrane, CLCM-C4: cross-linked collagen membrane.

integration. CLCM-C4 still exhibited slight tissue integration at this time point. As expected, NC did not present any signs of tissue integration at any time point.

Tissue ingrowth

At 4 weeks, all membranes showed a certain degree of tissue ingrowth except for CLCM-C4 and NC (Figure 3B and Table 1). While T1 showed marked tissue ingrowth, T2, T3, NCM-C3, PLGA-C1, and PLA-C2 displayed slight to moderate tissue ingrowth. At 13 weeks, the tissue ingrowth was higher than at 4 weeks, particularly in PLGA-C1 and PLA-C2, in which complete tissue ingrowth could be detected. In contrast, no meaningful changes in tissue ingrowth were observed in groups T1, T2, and NCM-C3. At 26 weeks, tissue ingrowth was completed in T1, NCM-C3, PLGA-C1, and PLA-C2, while T2, T3, and CLCM-C4 showed only slight signs of tissue integration. As expected, NC did not reveal any signs of tissue ingrowth, regardless of time point.



A

Figure 2. Degradation of the membranes over time. (A) Degradation scores of the different membranes. (B) Histological overview of the region of interest illustrating degradation at different time points. Modified Masson's trichrome staining (scale bar = 1 mm).

Data represent the means±standard deviations.

PLGA: poly(lactic-co-glycolic acid), PLA: poly(lactic acid), NC: negative control, T1: synthetic PLGA prototype test 1, T2: synthetic PLGA prototype test 2, T3: synthetic PLGA prototype test 3, PLGA-C1: commercially available PLGA membrane, PLA-C2: synthetic PLA membrane, NCM-C3: native collagen membrane, CLCM-C4: cross-linked collagen membrane, D: dermis, M: muscle layer, SC: subcutaneous. (continued to the next page)

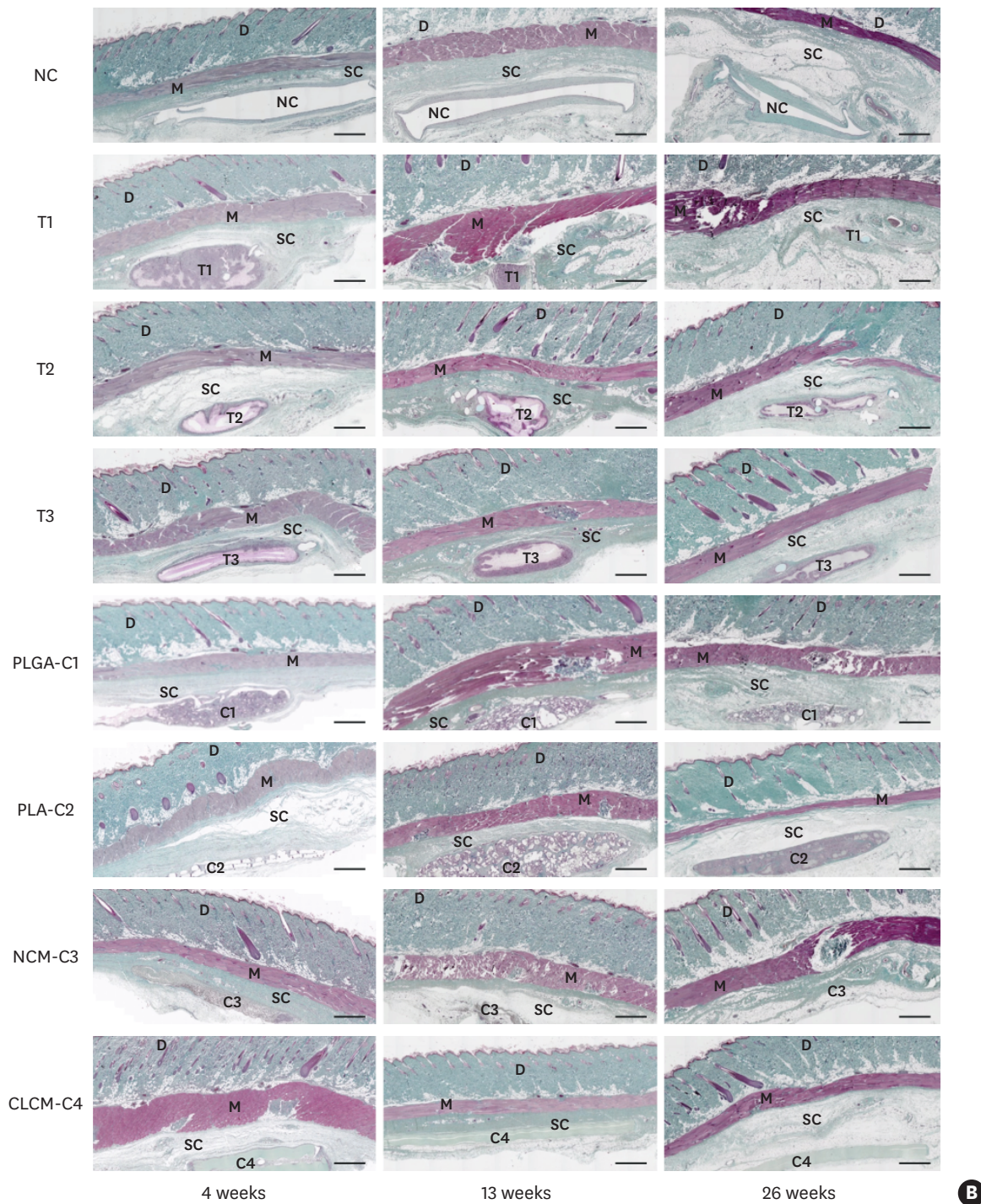


Figure 2. (Continued) Degradation of the membranes over time. (A) Degradation scores of the different membranes. (B) Histological overview of the region of interest illustrating degradation at different time points. Modified Masson's trichrome staining (scale bar = 1 mm). Data represent the means±standard deviations.

PLGA: poly(lactic-co-glycolic acid), PLA: poly(lactic acid), NC: negative control, T1: synthetic PLGA prototype test 1, T2: synthetic PLGA prototype test 2, T3: synthetic PLGA prototype test 3, PLGA-C1: commercially available PLGA membrane, PLA-C2: synthetic PLA membrane, NCM-C3: native collagen membrane, CLCM-C4: cross-linked collagen membrane, D: dermis, M: muscle layer, SC: subcutaneous.

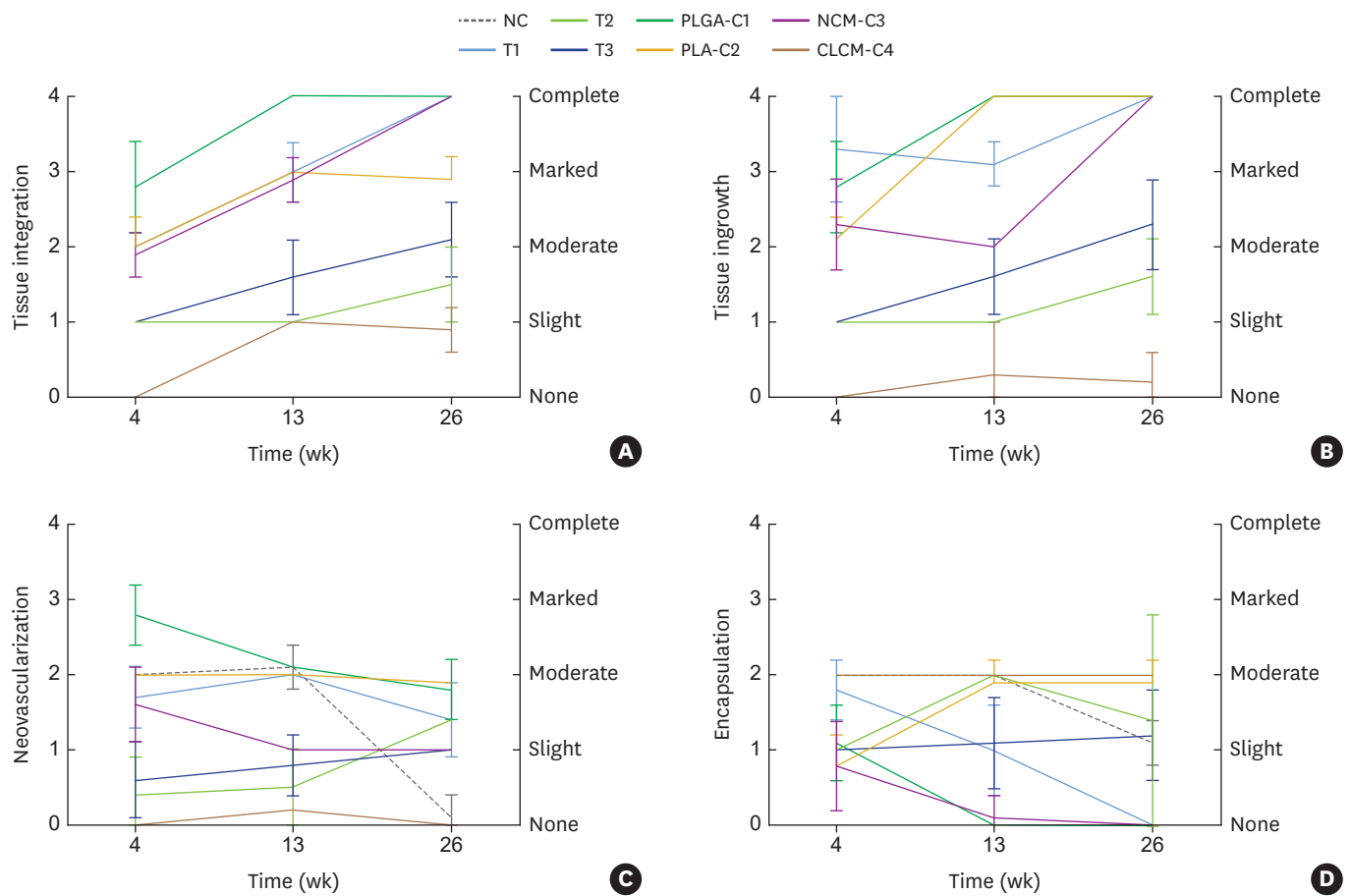


Figure 3. Local tissue reaction to the different membranes over time. (A) Tissue integration. (B) Tissue ingrowth. (C) Neovascularization. (D) Encapsulation. Data represent the means±standard deviations.

PLGA: poly(lactic-co-glycolic acid), PLA: poly(lactic acid), NC: negative control, T1: PLGA prototype test 1, T2: PLGA prototype test 2, T3: PLGA prototype test 3, PLGA-C1: commercially available PLGA membrane, PLA-C2: synthetic PLA membrane, NCM-C3: native collagen membrane, CLCM-C4: cross-linked collagen membrane.

Neovascularization

At 4 weeks, all but the CLCM-C4 membrane showed signs of vascularization (Figure 3C and Table 1). While PLGA-C1, PLA-C2, NCM-C3, T1, and NC generally displayed groups of 4–7 capillaries with supporting fibroblastic structures, T2, T3, and particularly CLCM-C4 displayed no to minimal capillary proliferation. At 13 weeks, the extent of vascularization was similar to that observed at 4 weeks in all membranes except CLCM-C4, which displayed only slight signs of vascularization. After a healing period of 26 weeks, T2 and T3 displayed higher vascularization than before, while the other membranes showed no clear changes compared to 13 weeks.

Encapsulation

At 4 weeks, all membranes displayed a slight degree of encapsulation except CLCM-C4 and NC, which showed moderate encapsulation (Figure 3D and Table 1). At 13 weeks, relative to 4 weeks, the degree of encapsulation was lower in T1, NCM-C3, and in PLGA-C1, while it was higher in T2 and PLA-C2. At 26 weeks, no signs of encapsulation were detectable in T1, NCM-C3, and PLGA-C1. In contrast, T2, T3, PLA-C2, and NC displayed slight to moderate

signs of encapsulation. CLCM-C4 did not show any changes compared to previous time points, exhibiting moderate encapsulation throughout.

Inflammation

At 4 weeks, the local inflammatory response was characterized by a small to moderate number of macrophages and giant cells admixed with a small number of polymorphonuclear cells (PMNs) and a few lymphocytes (Table 2). While NC, PLA-C2, and CLCM-C4 displayed only slight infiltration of macrophages, T1, T2, T3, and PLGA-C1 showed a moderate to marked macrophage presence. Moderate infiltration of giant cells was observed in all groups except NC and NCM-C3. A small number of PMNs were consistently found in all but 2 groups (CLCM-C4 and T1). The presence of lymphocytes did not substantially differ between the groups except for NCM-C3, which exhibited moderate lymphocyte infiltration. Notably, CLCM-C4 elicited the least robust inflammatory reaction of the groups (Figure 4).

At 13 weeks, histological analysis was used to demonstrate that the local inflammatory response was still characterized by a small to moderate number of macrophages (Table 2). The appearance of giant cells and lymphocytes in all groups was similar to that at 4 weeks. However, PMNs had almost disappeared at this time point and could not be detected in the NCM-C3, T1, and CLCM-C4 groups. Overall, these observations suggest a less robust inflammatory response than that observed at 4 weeks (Figure 4).

At 26 weeks, most groups displayed slight to moderate infiltration of macrophages, while PLA-C2 showed a marked macrophage presence (Table 2). In general, the extent of infiltration of giant cells was slight to moderate, except for NC, NCM-C3, and CLCM-C4, in which giant cells were barely visible or could not be detected. Regarding lymphocytes, their appearance did not differ substantially between the membranes and did not meaningfully change from 13 weeks of healing onward. PMNs were hardly present and could not be detected in the PLGA-C2, CLCM-C4, T1, or T3 groups. Although the inflammatory response at this time point was similar to that at 13 weeks of healing, it seemed to be lower than that at 4 weeks (Figure 4).

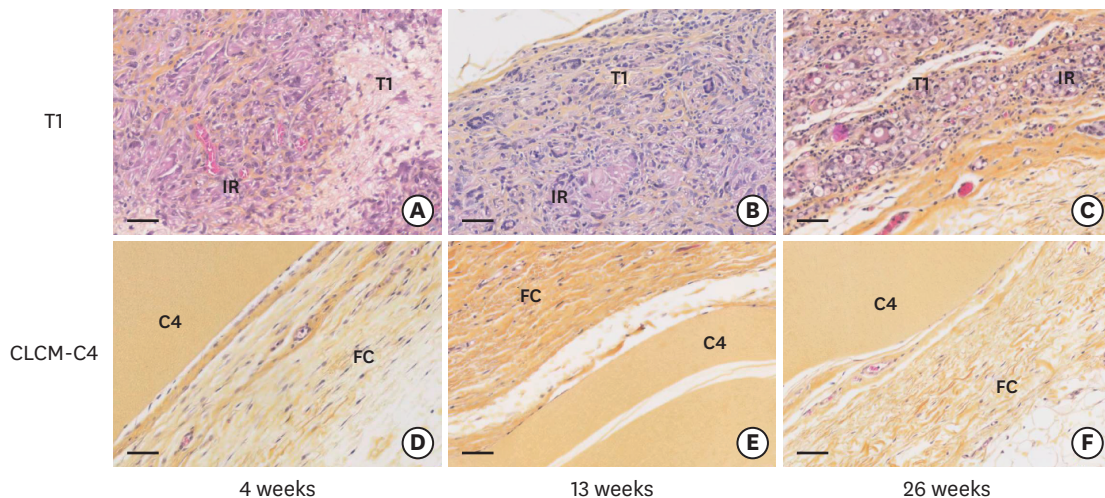


Figure 4. Inflammatory tissue reaction over time at the implantation sites. Representative histological images of 2 different membranes illustrating distinct inflammation at 4 (A, D), 13 (B, E) and 26 weeks (C, F) of healing (scale bar = 50 µm).
 PLGA: poly(lactic-co-glycolic acid), T1: synthetic PLGA prototype test 1, CLCM-C4: cross-linked collagen membrane, IR: inflammatory reaction, FC: fibrous capsule.

DISCUSSION

The present *in vivo* study investigating local tissue reactions and degradation of 3 PLGA membrane prototypes compared to commercially available resorbable membranes predominantly demonstrated the following: full integration of the barrier membranes into the host tissues within 13 weeks (PLGA-C1) and 26 weeks (T1 and NCM-C3) accompanied by fast tissue ingrowth; a minimal to low degradation rate of NCM-C3 and T1 at early time points, followed by a steeply increased degradation rate at 26 weeks; and a comparable inflammatory response across all non-cross-linked membranes.

The membranes indicated for GBR must fulfill a certain set of requirements. Apart from the basic barrier function, these requirements include biocompatibility, biodegradability, and integration with the host tissues [5,7]. In the present study, the prototype membrane T1, along with PLGA-C1 and NCM-C3, displayed the fastest tissue integration, with full integration at 26 weeks. The rapid tissue integration of the aforementioned membranes can be attributed to the materials used. T1 and PLGA-C1 are made of synthetic polymers that are biodegradable and highly biocompatible [18]. In a recent preclinical study, PLGA membranes already exhibited invasion by different cell types at 4 weeks [19], which is consistent with the fast tissue integration found with T1 and PLGA-C1 in the present study. The difference between T1 and PLGA-C1 and the other 2 PLGA prototypes (T2 and T3) may be explained by the different PLGA polymers used for their manufacture. Considering that T1 and T2 are both hydrophilic and that no considerable variation between T2 and T3 was observed, one might assume that the hydrophilic properties have no influence on the results. In contrast, NCM-C3 is made of collagen, a principal component of connective tissue, thereby explaining the excellent tissue integration. The good tissue integration observed with NCM-C3 in the present study aligns with the results of other studies [13,20]. In a preclinical *in vivo* study in rats, the biodegradation of different resorbable collagen membranes was investigated [13]. In that study, which had a similar design to the present study, NCM-C3 displayed more rapid tissue integration than did cross-linked membranes [13]. In contrast, a cross-linked collagen membrane (CLCM-C4, the same as in the present study) exhibited minimal tissue integration even at 26 weeks [13].

Adequate barrier integrity over time is a key quality of GBR membranes. In order to obtain predictable clinical outcomes, membranes must retain their function for a certain period of time [7]. T1 and NCM-C3 exhibited minimal to slight degradation at the earliest time point (4 weeks) and marked to complete degradation at 26 weeks. These results are consistent with previous findings indicating that collagen membranes degrade rapidly [20]. This degradation varies depending on the membrane tissue origin, the chemical cross-linking, and the implantation site [11]. Membrane degradation is based on numerous enzymes that are capable of breaking down collagen. For example, collagenases produced by *Porphyromonas gingivalis* have been shown to be capable of degrading collagen membranes [21]. This is of clinical relevance, since in case of premature membrane exposure and subsequent rapid degradation, clinical outcomes may be impaired [22]. As an option to counteract rapid degradation and to enhance the stability of collagen membranes, physiochemical cross-linking has been introduced. In the present study, cross-linked membranes displayed only minimal signs of degradation. Interestingly, the few observed signs of degradation were associated with the least robust inflammatory reaction of all investigated membranes, even when compared to the NC. These findings are in agreement with previous data showing a

low degradation rate for cross-linked membranes [20]. Such enhanced stability is commonly associated with low tissue integration levels. The latter may account for the higher rate of adverse events reported to be associated with cross-linked membranes [23]. Membrane exposure due to wound dehiscence can lead to insufficient bone regeneration [22]. PLGA copolymers, in contrast, degrade via hydrolysis [19]. The degradation times of PLGA copolymers vary depending on their glycolic acid content, molecular weight, and porosity [24]. These aspects may explain the differences in terms of degradation between the PLGA membranes used in the present study.

Although degradation time may influence clinical outcomes, an ideal membrane degradation time has not yet been established [7]. In fact, the evolution of membranes has been mainly driven by optimizing the barrier function and the ease of handling of different clinical scenarios, rather than by focusing on biology. It is therefore important to examine the inflammatory response to different membranes. In the present study, nearly all of the membranes elicited a similar inflammatory response, with peaks coinciding with degradation onset. The exception was the cross-linked membrane, which displayed no degradation during the entire study and a minimal inflammatory response at all time points, consistent with the slight cellular ingrowth observed in the present and previous studies [13]. One must bear in mind, however, that the inflammatory response was semi-quantitatively assessed using a grading system and without utilizing absolute values.

The present study does have limitations. The pouch model does not fully reflect the conditions of the oral cavity with the oral microbiome, which is expected to influence the reactions of the host tissue to the different membranes. Moreover, in a clinical scenario, resorbable membranes are stabilized with membrane-supporting material underneath, which may also modify the overall tissue response. This phenomenon could not be evaluated in the present model. Therefore, future studies in large animal models should be performed in order to examine whether the present findings have an impact in GBR procedures. In addition, and considering the emerging evidence that membranes are not just passive barriers, future studies should also evaluate the biological activity of the membranes. Finally, it is important to remark that only a descriptive statistical analysis was performed, which calls for caution when interpreting these findings.

In conclusion, 3 PLGA prototypes, particularly T1, induced favorable tissue integration, exhibited a similar degradation rate as native collagen membranes, and elicited a similar inflammatory response to commercially available non-cross-linked resorbable membranes. This inflammatory response seems to be associated with the degradation kinetics of the membrane, irrespective of their material composition.

ACKNOWLEDGEMENTS

The authors thank Lorenz Uebersax for collaborating in the preparation of the manuscript. The study was supported by a grant from Sunstar Suisse SA in Etoy, Switzerland and further supported by the Clinic of Reconstructive Dentistry at the University of Zurich, Switzerland.

REFERENCES

1. Bornstein MM, Halbritter S, Harnisch H, Weber HP, Buser D. A retrospective analysis of patients referred for implant placement to a specialty clinic: indications, surgical procedures, and early failures. *Int J Oral Maxillofac Implants* 2008;23:1109-16.
[PUBMED](#)
2. Khojasteh A, Kheiri L, Motamedian SR, Khoshkam V. Guided bone regeneration for the reconstruction of alveolar bone defects. *Ann Maxillofac Surg* 2017;7:263-77.
[PUBMED](#) | [CROSSREF](#)
3. Hämmerle CH, Jung RE. Bone augmentation by means of barrier membranes. *Periodontol* 2000 2003;33:36-53.
[PUBMED](#) | [CROSSREF](#)
4. Omar O, Elgali I, Dahlin C, Thomsen P. Barrier membranes: more than the barrier effect? *J Clin Periodontol* 2019;46 Suppl 21:103-23.
[PUBMED](#) | [CROSSREF](#)
5. Dahlin C, Linde A, Gottlow J, Nyman S. Healing of bone defects by guided tissue regeneration. *Plast Reconstr Surg* 1988;81:672-6.
[PUBMED](#) | [CROSSREF](#)
6. Retzepi M, Donos N. Guided bone regeneration: biological principle and therapeutic applications. *Clin Oral Implants Res* 2010;21:567-76.
[PUBMED](#) | [CROSSREF](#)
7. Sanz M, Dahlin C, Apatzidou D, Artzi Z, Bozic D, Calciolari E, et al. Biomaterials and regenerative technologies used in bone regeneration in the craniomaxillofacial region: consensus report of group 2 of the 15th European Workshop on Periodontology on Bone Regeneration. *J Clin Periodontol* 2019;46 Suppl 21:82-91.
[PUBMED](#) | [CROSSREF](#)
8. Chiapasco M, Zaniboni M. Clinical outcomes of GBR procedures to correct peri-implant dehiscences and fenestrations: a systematic review. *Clin Oral Implants Res* 2009;20 Suppl 4:113-23.
[PUBMED](#) | [CROSSREF](#)
9. McAllister BS, Haghghat K. Bone augmentation techniques. *J Periodontol* 2007;78:377-96.
[PUBMED](#) | [CROSSREF](#)
10. Zitzmann NU, Naef R, Schärer P. Resorbable versus nonresorbable membranes in combination with Bio-Oss for guided bone regeneration. *Int J Oral Maxillofac Implants* 1997;12:844-52.
[PUBMED](#)
11. Bunyaratavej P, Wang HL. Collagen membranes: a review. *J Periodontol* 2001;72:215-29.
[PUBMED](#) | [CROSSREF](#)
12. Elgali I, Omar O, Dahlin C, Thomsen P. Guided bone regeneration: materials and biological mechanisms revisited. *Eur J Oral Sci* 2017;125:315-37.
[PUBMED](#) | [CROSSREF](#)
13. Rothamel D, Schwarz F, Sager M, Hertzen M, Sculean A, Becker J. Biodegradation of differently cross-linked collagen membranes: an experimental study in the rat. *Clin Oral Implants Res* 2005;16:369-78.
[PUBMED](#) | [CROSSREF](#)
14. Lee SW, Kim SG. Membranes for the guided bone regeneration. *Maxillofac Plast Reconstr Surg* 2014;36:239-46.
[PUBMED](#) | [CROSSREF](#)
15. Hutmacher D, Hürzeler MB, Schliephake H. A review of material properties of biodegradable and bioresorbable polymers and devices for GTR and GBR applications. *Int J Oral Maxillofac Implants* 1996;11:667-78.
[PUBMED](#)
16. von Arx T, Broggin N, Jensen SS, Bornstein MM, Schenk RK, Buser D. Membrane durability and tissue response of different bioresorbable barrier membranes: a histologic study in the rabbit calvarium. *Int J Oral Maxillofac Implants* 2005;20:843-53.
[PUBMED](#)
17. Thoma DS, Nänni N, Benic GI, Weber FE, Hämmerle CH, Jung RE. Effect of platelet-derived growth factor-BB on tissue integration of cross-linked and non-cross-linked collagen matrices in a rat ectopic model. *Clin Oral Implants Res* 2015;26:263-70.
[PUBMED](#) | [CROSSREF](#)
18. Makadia HK, Siegel SJ. Poly lactic-co-glycolic acid (PLGA) as biodegradable controlled drug delivery carrier. *Polymers (Basel)* 2011;3:1377-97.
[PUBMED](#) | [CROSSREF](#)

19. Hoornaert A, d'Arros C, Heymann MF, Layrolle P. Biocompatibility, resorption and biofunctionality of a new synthetic biodegradable membrane for guided bone regeneration. *Biomed Mater* 2016;11:045012.
[PUBMED](#) | [CROSSREF](#)
20. Rothamel D, Benner M, Fienitz T, Happe A, Kreppel M, Nickenig HJ, et al. Biodegradation pattern and tissue integration of native and cross-linked porcine collagen soft tissue augmentation matrices - an experimental study in the rat. *Head Face Med* 2014;10:10.
[PUBMED](#) | [CROSSREF](#)
21. Sela MN, Kohavi D, Krausz E, Steinberg D, Rosen G. Enzymatic degradation of collagen-guided tissue regeneration membranes by periodontal bacteria. *Clin Oral Implants Res* 2003;14:263-8.
[PUBMED](#) | [CROSSREF](#)
22. Thoma DS, Bienz SP, Figuero E, Jung RE, Sanz-Martin I. Efficacy of lateral bone augmentation performed simultaneously with dental implant placement: a systematic review and meta-analysis. *J Clin Periodontol* 2019;46 Suppl 21:257-76.
[PUBMED](#) | [CROSSREF](#)
23. Annen BM, Ramel CF, Hämmerle CH, Jung RE. Use of a new cross-linked collagen membrane for the treatment of peri-implant dehiscence defects: a randomised controlled double-blinded clinical trial. *Eur J Oral Implantology* 2011;4:87-100.
[PUBMED](#)
24. Lu L, Peter SJ, Lyman MD, Lai HL, Leite SM, Tamada JA, et al. *In vitro* and *in vivo* degradation of porous poly(DL-lactic-co-glycolic acid) foams. *Biomaterials* 2000;21:1837-45.
[PUBMED](#) | [CROSSREF](#)